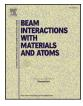
Contents lists available at ScienceDirect



Nuclear Inst. and Methods in Physics Research B

journal homepage: www.elsevier.com/locate/nimb



# Ab initio modelling of the Y, O, and Ti solute interaction in fcc-Fe matrix



A. Gopejenko<sup>a</sup>, Yu.A. Mastrikov<sup>a</sup>, Yu.F. Zhukovskii<sup>a</sup>, E.A. Kotomin<sup>a,\*</sup>, P.V. Vladimirov<sup>b</sup>, A. Möslang<sup>b</sup>

<sup>a</sup> Institute of Solid State Physics, University of Latvia, Kengaraga 8, Riga, LV 1063, Latvia

<sup>b</sup> Karlsruhe Institute of Technology, Institute for Materials Research-1, P.O. Box 3640, 76021 Karlsruhe, Germany

ARTICLEINFO	A B S T R A C T				
Keywords: ODS steel Yttria nanoparticles Density functional calculations Energetic interactions	Strengthening of the ODS steels by $Y_2O_3$ precipitates permits to increase their operation temperature and ra- diation resistance, which is important in construction materials for future fusion and advanced fission reactors. Both size and spatial distribution of oxide particles significantly affect mechanical properties and radiation resistance of ODS steels. Addition of the Ti species (present also as a natural impurity atoms in iron lattice) in the particles of $Y_2O_3$ powder before their mechanical alloying leads to the formation of YTiO <sub>3</sub> , $Y_2TiO_5$ , and $Y_2Ti_2O_7$ nanoparticles in ODS steels. Modelling of these nanoparticle formation needs detailed knowledge of the en- ergetic interactions between ions. We have performed detailed first principles calculations of the interactions between two Y and O atoms, two Ti and O atoms as well as between Y, Ti, and O atoms which will be used in further kinetic Monte Carlo modelling of the nanoparticle formation.				

### 1. Introduction

Reduced activation ferritic-martensitic (RAFM) steels have been developed in 1950s and are considered as promising structural materials for future fusion reactors [1,2]. Further development of the oxide dispersed strengthened (ODS) alloys steel as structure material for nuclear power plants (NPP) noticeably increases its mechanical, radiation and thermal stability, e.g., in fast breeder reactors [3]. The modern generation of RAFM steels strengthened by oxide particles allows increasing the operation temperature of the fusion reactors by 100 °C (achieving up to 650 °C), thus markedly improving their efficiency [3,4]. Y<sub>2</sub>O<sub>3</sub>, which is one of the most stable oxides, has proved to be one of the most suited oxides to strengthen RAFM steels, e.g., ODS-Eurofer. Its melting temperature is higher than that of the RAFM steels, which might play an important role in the formation of the oxide particles. ODS steels are usually produced by mechanical alloying for several tens of hours followed by a hot isostatic pressing (hipping) at temperature around 1000–1200 °C and pressure  $\sim$  100 MPa.

There is an experimental evidence that a significant fraction of Y and O atoms exist in a steel matrix in concentrations above their equilibrium solubility [5,6]. This suggests that the *precipitation* of  $Y_2O_3$  particles might occur already during the hipping stage [7]. The size of  $Y_2O_3$  nanoparticles is found to be within the range of 3 to 45 nm. (Note that the nanoparticles with the size of 3 nm are the smallest particles that could be found when using transmission electron microscopy

(TEM) [8]). The small nanoparticles usually possess a spherical shape, while the particles exceeding 12 nm demonstrate a well-established faceted surface [9]. The TEM study reveals that ODS particles have a complex structure [10] with the core comprised of the  $(Y_{1.8}Mn_{0.2})O_3$  phase, which possesses a typical cubic  $Y_2O_3$  structure.

Both the size and spatial distribution of the oxide particles significantly affect the mechanical properties of the ODS as well as its radiation resistance. Thus, the ability to control the structure/composition of the oxide nanoparticles and the minimisation of their size are important for improving the properties of the material. In particular, ODS steels with 0.3 wt% Ti concentration were studied earlier [11–14]. Enhanced Ti concentration leading to the subsequent formation of Y-Ti-O oxides effectively reduces the oxide particle size, resulting in the growth of cluster density, which might have an important role in pinning the dislocations and improving mechanical properties of ODS steels [11]. The presence of numerous Y-Ti-O oxide particles such as YTiO<sub>3</sub>, Y<sub>2</sub>TiO<sub>5</sub> and Y<sub>2</sub>Ti<sub>2</sub>O<sub>7</sub> with a uniform spatial distribution was reported in Ref. [12]. The striking effect of Ti on particle size refinement has been observed with the optimal Ti concentration of 0.3 wt% [13]. The oxide average size was found to be  $11 \pm 6 \text{ nm}$  in ODS Eurofer,  $10 \pm 3 \text{ nm}$  in 13.5Cr-ODS and  $5 \pm 2 \text{ nm}$  in 13.5Cr-0.3Ti ODS. After irradiation the average size of the oxide particles in ODS Eurofer and 13.5Cr ODS decreases, while the oxide particle size and the chemical composition of the clusters remains stable in 13.5Cr-0.3Ti ODS [14].

https://doi.org/10.1016/j.nimb.2018.07.033

<sup>\*</sup> Corresponding author.

E-mail address: kotomin@latnet.lv (E.A. Kotomin).

Received 30 October 2017; Received in revised form 13 July 2018; Accepted 30 July 2018 0168-583X/ © 2018 Elsevier B.V. All rights reserved.

Y<sub>2</sub>O<sub>3</sub> crystal possesses a cubic structure with the lattice parameter of 10.604 Å whereas the Y-O bond lengths reported in Refs. [15,16] are qualitatively close and vary from 2.24 Å to 2.33 Å. As to TiO<sub>2</sub>, it is produced from ilmenite (FeTiO<sub>3</sub>) with the rhombohedral crystal structure and the lattice parameters of a = 5.0875 Å and c = 14.0827 Å [17]. The most widespread anatase and rutile phases of titania possess the tetragonal crystal structure with lattice parameters of a = 3.3845 Å and c = 9.5143 Å as well as a = 4.5937 Å and c = 2.9587 Å, respectively.

The calculated Ti-O bond lengths in anatase and rutile forms of TiO<sub>2</sub> are also similar being equal to 1.93 Å and 1.98 Å as well as 1.95 Å and 1.98 Å, respectively [18]. Titania can also form less-stable brookite phase possessing orthorhombic crystal structure and the lattice parameters of a = 5.4558 Å, b = 9.1819 Å and c = 5.1429 Å [19]. In the present study, we have performed large-scale first-principles modelling of various configurations of triple-wise Y-O-Y, Y-O-Ti and Ti-O-Ti defect clusters, with the focus on the binding energies between the defect atoms, the electron charge transfer and the difference electron charge density (ECHD), as well as the displacements of the defect atoms, which is the first step to the kinetic Monte Carlo (kMC) modelling of the nanoparticle formation in ODS.

#### 2. Modelling details

Ab initio calculations have been performed using the VASP 5.3 computer code [20]. Some of the defect configurations that were reported earlier [21-24] were recalculated and the modelling results have been compared with those obtained using previous versions of VASP computer code (4.6 and 5.2). It is based on the Density Functional Theory (DFT) approach with a plane-wave (PW) basis set [20,25] and Perdew-Wang-91 GGA [26] non-local exchange-correlation functional, which operates with Fe core electrons of  $(4s^13d^7$  outer shell), O  $(2s^22p^4)$ , Y  $(4s^24p^65s^14d^2)$ , and Ti  $(3p^64s^23d^4)$  atoms with 8, 6, 11, and 12 external electrons, respectively. The core electrons are described within the Projector-Augmented Wave (PAW) method [27] and have been treated with PAW-PW91 pseudopotentials. We consider here the fcc structured iron lattice, which is stable under hipping conditions at high temperatures, when the magnetic moments of Fe atoms are disordered; this allows us to describe the iron crystal as paramagnetic [24].

A number of different test calculations has been performed, in order to define the calculation parameters required to achieve plausible results and to reproduce basic experimental data for fcc-Fe lattice, such as lattice constant a<sub>0</sub>, bulk modulus, cohesive energy per atom E<sub>coh</sub>, etc. The test calculations have also included the analysis of the convergence of the results depending on the supercell size, the cut-off energy as well as the k-point set in the corresponding Brillouin zone. The supercell used in these calculations is chosen to be cubic, with the  $4a_0 \times 4a_0 \times 4a_0$  extension containing 64 atoms. The calculated optimized lattice constant has been found to be 3.45 Å (cf. 3.4-3.6 Å [21]). The test calculations showed that the k-point sets in the Brillouin zone (BZ) should be at least  $7 \times 7 \times 7 k$ -mesh for supercell, the Brillouin zone has been sampled  $9 \times 9 \times 9$  using the Monkhorst-Pack scheme [28]. The cut-off energy required to achieve the plausible results was found to be 800 eV [21-24]. The lattice parameters optimised for the perfect fcc-Fe have been used for the further calculations of the defect configurations in fcc iron.

For arbitrary configurations of defective iron supercells, positions of all atoms have been determined by a minimization of the total energy. The effective atomic charges have been estimated using the Bader topological analysis [29]. The relative atom displacements have been calculated using rdf.pl script available in the VASP TST tools [30] containing source code and scripts for finding saddle points and evaluating transition state theory (TST) rate constants. The chosen computational model has been verified for the key properties of the perfect  $\gamma$ -Fe single crystal determined earlier both experimentally and

Table 1 Calculated parameters for two  $Y_{\rm Fe}$  and one  $O_{\rm Fe}$  atoms.

Configuration	<i>E<sub>bind</sub></i> , eV	∆q, e <sup>*</sup> (Y <sub>Fe</sub> )	Δq, e <sup>*</sup> (Y <sub>Fe</sub> )	$\Delta q, e^*$ (O <sub>Fe</sub> )	<i>δr</i> <sub>Y</sub> (1), Å	<i>δr</i> <sub>Y</sub> (2), Å	δr <sub>o</sub> , Å
1NN**	1.12	1.06	1.08	-1.16	0.27	0.27	0.64
2NN**	2.00	1.17	1.17	-1.19	0.36	0.36	0.64
3NN**	2.20	1.23	1.23	-1.19	0.45	0.45	0.60

\* Estimated within the Bader topological analysis [29].

\*\* Distance between two Y<sub>Fe</sub> atoms, while O<sub>Fe</sub> is the 1NN to both Y atoms.

theoretically [31–36]. The equilibrium lattice constant, bulk modulus and cohesive energy for a cubic paramagnetic  $\gamma$ -Fe lattice have been calculated to be (*i*) 3.44 Å, (*ii*) 162 GPa and (*iii*) 4.96 eV/atom, respectively. Obtained results are in a reasonable agreement with other *ab initio* calculations on  $\gamma$ -Fe iron: (*i*) 3.40–3.60 Å [31,32,34], (*ii*) 171–211 GPa [31,33] and (*iii*) 4.42 eV/atom [33], respectively. The same is true for the relevant experimental values: (*i*) 3.57 Å [35], (*ii*) 133–164 GPa [36], both obtained for  $\gamma$ -Fe as well as (*iii*) 4.28 eV/atom [34] for a low-temperature ferromagnetic  $\alpha$ -Fe which is believed to be close to cohesive energy of  $\gamma$ -Fe.

### 3. Results and discussion

Both the Bader charges and relative atomic displacements have been calculated and analysed for a number of models described below. The results systematized in Table 1 correspond to the schematic models shown in Fig. 1a-c. The OFFe atom has been positioned as the first nearest neighbour (1NN) to both Y<sub>Fe</sub> atoms in all cases. It is important to note that the size of Y atom is larger than that of Fe atoms, which leads to the expansion of the coordination spheres around the Y<sub>Fe</sub> atoms. A noticeable O<sub>Fe</sub> atom displacement occurs during the relaxation of all three calculated configurations. The expansion of the coordination spheres around Y<sub>Fe</sub> atoms noticeably pushes a smaller O<sub>Fe</sub> atom away from both  $Y_{Fe}$  atoms by 0.24 Å, while the distance between  $Y_{Fe}$  atoms increases by 0.14 Å in the 1NN configuration (Fig. 1a and Table 1). OFFe is pushed away from both  $Y_{Fe}$  atoms by 0.13 Å towards Fe atoms, while the distance between two 2NN Y<sub>Fe</sub> atoms decreases by 0.42 Å (Fig. 1b and Table 1). In the 3NN configuration, the distance between O<sub>Fe</sub> and both  $Y_{Fe}$  atoms decreases by 0.09 Å, while the distance between the two  $Y_{Fe}$ atoms is almost unchanged (the latter become closer by 0.01 Å). The described atom displacements can explain the values of the binding energies. The smallest binding energy has been found between the defects when they are positioned as 1NN, the binding energies increased with the increase of the distance between the two  $Y_{Fe}$  atoms with the largest binding energy of  $2.20\,eV$  calculated for the 3NN configuration (Fig. 1c and Table 1). The Bader analysis shows that  $Y_{Fe}$ atoms donate 1.06-1.23 e, while O atom attracts 1.16-1.19 e.

The results of the calculations on the unit cells configurations shown in Fig. 2a and 2b are presented in Table 2. The atom displacements for the configuration where Y<sub>Fe</sub> atom is positioned as 1NN are qualitatively similar to those observed for the configurations with Y<sub>Fe</sub>-O<sub>Fe</sub>-Y<sub>Fe</sub>, *i.e.*, in this case both Y<sub>Fe</sub> atoms expand the coordination sphere around themselves pushing OFe atom away increasing the distance between OFe and both  $Y_{Fe}$  atoms by 0.45 Å, while the distance between two  $Y_{Fe}$ atoms increases by 0.38 Å. However, the results of calculations on the configuration when Y<sub>Fe</sub> atoms are placed as 2NN are different from those described above. This difference originates from the position of  $O_{\text{oct}}$  atom and the forces acting on it during the relaxation. In this configuration, Ooct atom is positioned symmetrically relatively to both yttrium atoms in the first coordination sphere and the forces from the Fe and Y atoms located in the first coordination sphere around Ooct are compensating each other. This results in no displacement of O<sub>oct</sub> atom in relation to its initial position during the relaxation. At the same time, both  $Y_{Fe}$  atoms are displaced away from  $O_{Fe}$  atom by 0.34 Å and by 0.69 Å from each other. No binding energies have been found between Download English Version:

# https://daneshyari.com/en/article/8039034

Download Persian Version:

https://daneshyari.com/article/8039034

Daneshyari.com